5+ model EABE : 1997 Prod.Type:FTP pp.1–12(col.fig.:NIL) ED:Dibyendu PAGN:Bhaskara SCAN:

ARTICLE IN PRESS

ELSEVIER

Engineering Analysis with Boundary Elements ▮ (▮▮▮▮) ▮▮▮–▮▮▮

ENGINEERING ANALYSIS with BOUNDARY ELEMENTS

www.elsevier.com/locate/enganabound

Topology optimization of 2D elastic structures using boundary elements

Luis Carretero Neches[a], Adrián P. Cisilino[b,*]

[a]*Grupo de Elasticidad y Resistencia de Materiales, Departamento de Mecánica del Continuo, Escuela de Ingenieros Industriales, Universidad de Sevilla, Avda. de los Descubrimientos s/n, E-41092 Sevilla, Spain*

[b]*División Soldadura y Fractomecánica, INTEMA, Facultad de Ingeniería, Universidad Nacional de Mar del Plata, Av. Juan B. Justo 4302, (7600) Mar del Plata, Argentina*

Received 6 August 2007; accepted 11 October 2007

Abstract

Topological optimization provides a powerful framework to obtain the optimal domain topology for several engineering problems. The topological derivative is a function which characterizes the sensitivity of a given problem to the change of its topology, like opening a small hole in a continuum or changing the connectivity of rods in a truss.

A numerical approach for the topological optimization of 2D linear elastic problems using boundary elements is presented in this work. The topological derivative is computed from strain and stress results which are solved by means of a standard boundary element analysis. Models are discretized using linear elements and a periodic distribution of internal points over the domain. The total potential energy is selected as cost function. The evaluation of the topological derivative is performed as a post-processing procedure. Afterwards, material is removed from the model by deleting the internal points and boundary nodes with the lowest values of the topological derivate. The new geometry is then remeshed using a weighted Delaunay triangularization algorithm capable of detecting "holes" at those positions where internal points and boundary points have been removed. The procedure is repeated until a given stopping criterion is satisfied.

The proposed strategy proved to be flexible and robust. A number of examples are solved and results are compared to those available in the literature.

Keywords: Topology optimization; Topological derivative; Boundary elements; Elastostatics

1. Introduction

Structural optimization is a major concern in the design of mechanical systems. The classical problem in engineering design consists in finding the optimum geometric configuration of a body that maximizes or minimizes a given cost function while it satisfies the problem boundary conditions. During the last 20 years a number of numerical techniques have been developed to solve the problem efficiently.

Following Ceá et al. [1], structural optimization techniques can be classified as follows:

- *Size optimization*: Only the cross sections of the structure are optimized. This approach is specially suited for the optimization of beam/bar structures.
- *Shape optimization*: The optimal geometry is searched within a class of domains having the same topology as the initial design, i.e., no holes are introduced in the optimization domain.
- *Topology optimization*: The shape and connectivity of the domain are both design variables; the introduction of new boundary is permitted via the creation of holes. This versatile approach is capable of delivering optimal designs with *a priori* poor information on the optimal shape of the structure, and it possess the ability of producing the best overall structure [2].

Homogenization methods are possibly the most used approach for topology optimization [3]. In these methods a

*Corresponding author. Tel.: +54 223 4816600x186; fax: +54 223 4810046.

E-mail address: cisilino@fi.mdp.edu.ar (A. Cisilino).

0955-7997/$ - see front matter © 2007 Published by Elsevier Ltd.
doi:10.1016/j.enganabound.2007.10.003

material model with micro-scale voids is introduced and the topology optimization problem is defined by seeking the optimal porosity of such a porous medium using one of the optimality criteria. In this way, the homogenization technique is capable of producing internal holes without prior knowledge of their existence. However, the homogenization method often produces designs with infinitesimal pores that make the structure not manufacturable. A number of variations of the homogenization method have been investigated to deal with these issues, such as penalization of intermediate densities and filtering procedures [4]. On the other hand, there exist the so-called level set methods which are based on the moving of free boundaries [5,6]. Although very effective, the main drawback of level set methods is the need of pre-existent holes within the model domain in order to conduct a topology optimization.

The topological derivative provides an alternative approach for shape optimization. It was firstly introduced by Ceá et al. [7] by combining a fixed point method with the natural extension of the classical shape gradient. The basic idea behind the topological derivative is the evaluation of cost function sensitivity to the creation of a hole. In this way, wherever this sensitivity is low enough (or high enough depending on the nature of the problem) the material can be progressively eliminated. Topological derivative methods aim to solve the aforementioned limitations of the homogenization methods.

A numerical approach for the topological optimization of 2D elastic problems using boundary elements is presented in this work. The formulation of the problem is based on the results by Novotny et al. [8], who introduced a new procedure for computing the topological derivative which allows overcoming some mathematical difficulties involved in its classical definition. The boundary element analysis is done using a standard direct formulation. Models are discretized using linear elements and a periodic distribution of internal points over the domain. The total strain energy is selected as cost function. Afterwards, material is removed from the model by deleting the internal points with the lowest (or highest) values of the topological derivate. The new geometry is remeshed using an extended Delaunay tessellation algorithm capable of detecting "holes" at those positions where internal points and nodes have been removed. In this way, the procedure avoids using intermediate densities, the classical limitation of the homogenization methods. The procedure is repeated until a given stopping criterion is satisfied. The performance of the proposed strategy is illustrated for a number of examples and their results compared to solutions available in the literature.

Although the FEM has been the main numerical tool for the implementation of topology optimization techniques, there are implementations using BEM (see Ref. [9]) and free boundary parametrization methods [6]. To the authors' knowledge, the only antecedent in the implementation of the Novotny et al. [8] approach for the computation of the topological derivative using BEM are the recent works by Cisilino [10] and Marckzak [11] for potential problems and by Marckzak [12] for elastic problems. Both implementations, that due to Marckzak [11,12] and the one presented in Ref. [10] use similar procedures for the computation of the topological derivative results. However, they differ in the strategy proposed for the creation of the holes and the model update and remeshing. The procedures introduced in Ref. [10] for potential problems are extended here to elasticity problems.

2. Topological sensitivity analysis

The original definition of the topological derivative, D_T, relates the sensitivity of a cost function $\psi(\Omega)$ when the topology of the optimization domain Ω is altered by creating a small cavity or hole. However, the direct application and implementation of this concept is not straightforward, as it is not possible to establish a homeomorphism between the domains with different topologies (domains with and without the hole).

Novotny et al. [8] proposed an alternative definition of the D_T that overcomes the problem. They assimilated the creation of a hole to the perturbation of a pre-existing hole whose radius tends to zero (see Fig. 1). Therefore, both topologies of the optimization domain Ω are now similar and it is possible to establish a homeomorphism between them. According to this new definition, the expression for the D_T is

$$D_T(x) = \lim_{\substack{\varepsilon\to 0\\ \delta\varepsilon\to 0}} \frac{\psi(\Omega_{\varepsilon+\delta\varepsilon}) - \psi(\Omega_\varepsilon)}{f(\varepsilon+\delta\varepsilon) - f(\varepsilon)}, \tag{1}$$

where $\psi(\Omega_\varepsilon)$ and $\psi(\Omega_{\varepsilon+\delta\varepsilon})$ are the cost function evaluated for the reference and perturbed domain, ε is the initial radius of the hole, $\delta\varepsilon$ is a small perturbation of the hole radius and f is a regularization function. The function f is problem dependant and $f(\varepsilon)\to 0$ when $(\varepsilon)\to 0$.

It could be argued that the new definition of the D_T in Eq. (1) merely provides the sensitivity of the problem when the size of the hole is perturbed and not when it is effectively created (as one has in the original definition of the topological derivative). However, it is understood that to expand a hole of radius ε, when $\varepsilon\to 0$, is nothing more than creating it (a complete mathematical proof that establishes the relation between both definitions of the D_T is given in Ref. [8]). Moreover, the relationship between the two definitions constitutes the formal relation between the D_T and the shape sensitivity analysis. The advantage of the novel definition for the topological derivative given by Eq. (1) is that the whole mathematical framework developed for the shape sensitivity analysis can now be used to compute the D_T.

Please cite this article as: Carretero Neches L, Cisilino A. Topology optimization of 2D elastic structures using boundary.... Eng Anal Bound Elem (2007), doi:10.1016/j.enganabound.2007.10.003

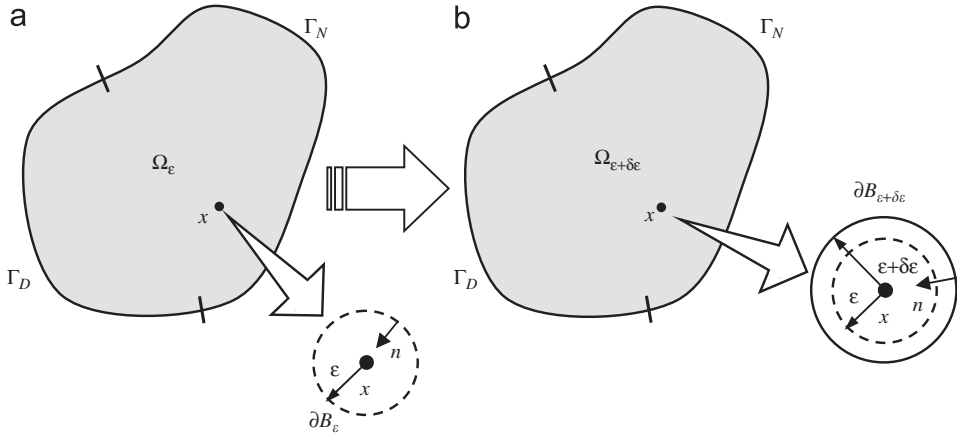

Fig. 1. New definition of the D_T as proposed by Novotny et al. [8]: (a) original domain with pre-existing hole $\psi(\Omega_\varepsilon)$ and (b) perturbed domain $\psi(\Omega_{\varepsilon+\delta\varepsilon})$.

3. The topological derivative for elasticity problems

In the present work the D_T is applied to the optimization of two-dimensional elastostatics. Following Novotny et al. [8,13], the topological derivative equations are briefly reviewed next, considering a mechanical model restricted to infinitesimal strains and displacements with a linear isotropic constitutive relation.

Let Ω_ε be the domain of a deformable body with a small hole with boundary ∂B_ε. The boundary $\Gamma_\varepsilon = \Gamma_N \cup \Gamma_D \cup \partial B_\varepsilon$ is submitted to a set of surface tractions $\bar{t}$ on the Neumann boundary Γ_N and displacement constraints on the Dirichlet boundary Γ_D. An homogeneous Neumann condition $\bar{t} = 0$ is imposed on the hole boundary ∂B_ε. Then, in absence of body forces the mechanical model can be described using the following variational formulation in terms of the displacement field u_ε: find u_ε: find u_ε such that

$$\int_{\Omega_\varepsilon} \sigma_\varepsilon(u_\varepsilon)\varepsilon_\varepsilon(w_\varepsilon)\,\mathrm{d}\Omega_\varepsilon = \int_{\Gamma_N} \bar{t}\cdot w_\varepsilon\,\mathrm{d}\Gamma_\varepsilon, \tag{2}$$

where w_ε is a field of admissible displacement variations which satisfies the condition $w_\varepsilon = 0$ on Γ_D; and σ_ε and ε_ε are the stress and strain fields, respectively.

The boundary-value problem given in Eq. (2) for the reference configuration Ω_ε, must also be satisfied in the perturbed configuration $\Omega_{\varepsilon+\delta\varepsilon}$ (see Section 2). In this way the variational formulation for the perturbed configuration is

$$\int_{\Omega_{\varepsilon+\delta\varepsilon}} \sigma_{\varepsilon+\delta\varepsilon}(u_{\varepsilon+\delta\varepsilon})\varepsilon_{\varepsilon+\delta\varepsilon}(w_{\varepsilon+\delta\varepsilon})\,\mathrm{d}\Omega_{\varepsilon+\delta\varepsilon} = \int_{\Gamma_N} \bar{t}\cdot w_{\varepsilon+\delta\varepsilon}\,\mathrm{d}\Gamma_{\varepsilon+\delta\varepsilon}, \tag{3}$$

where it has been assumed that the external loads remain fixed during the shape change.

The cost function $\psi(\Omega)$ is, in a certain way, arbitrary. For the case of elasticity problems the total strain energy can be adopted. The expression of the total strain energy for the reference domain is

$$\psi(\Omega_\varepsilon) = \frac{1}{2}\int_{\Omega_\varepsilon} \sigma_\varepsilon(u_\varepsilon)\varepsilon_\varepsilon(u_\varepsilon)\,\mathrm{d}\Omega_\varepsilon - \int_{\Gamma_N} \bar{t}u_\varepsilon\,\mathrm{d}\Gamma_\varepsilon, \tag{4}$$

where the domain integral in the right-hand side represents the total strain energy stored in the body and the boundary integral represents the external work. This objective function is equivalent to optimize the mean compliance of the problem.

The optimization problem can be stated as the minimization of the total potential energy (4) with the weak (variational) form of the state equations (2) and (3) as constraints. All these three equations can be used to derive the expression for the D_T using Eq. (1). This result was obtained by Novotny et al. [8] using Reynold's transport theorem and the concept of material derivatives of spatial fields:

$$D_T(x) = \lim_{\varepsilon\to 0}\frac{1}{f(\varepsilon)}\int_{\partial B_\varepsilon}\frac{1}{2}\sigma_\varepsilon(u_\varepsilon)\varepsilon_\varepsilon(u_\varepsilon)\,\mathrm{d}\partial B_\varepsilon. \tag{5}$$

Finally, an asymptotic analysis is performed in order to know the behaviour of the displacement solution u_ε, as well as the associated strain and stress fields, σ_ε and ε_ε, when $\varepsilon \to 0$. From this asymptotic analysis the final expression for the D_T in the original domain Ω (without the hole) are obtained:

$$D_T(x) = \frac{2}{1+\nu}\boldsymbol{\sigma}\cdot\boldsymbol{\varepsilon} + \frac{3\nu-1}{2(1-\nu^2)}tr\,\boldsymbol{\sigma}\,tr\,\boldsymbol{\varepsilon} \tag{6}$$

for plane stress and

$$D_T(x) = 2(1-\nu)\boldsymbol{\sigma}\cdot\boldsymbol{\varepsilon} + \frac{(1-\nu)(4\nu-1)}{2(1-2\nu)}tr\,\boldsymbol{\sigma}\,tr\,\boldsymbol{\varepsilon} \tag{7}$$

for plane strain.

The symbol ν in expressions (6) and (7) stand for the Poisson ratio, while $tr\,\boldsymbol{\sigma}$ and $tr\,\boldsymbol{\varepsilon}$ stand for the trace of the stress and strain tensors, respectively.

Please cite this article as: Carretero Neches L, Cisilino A. Topology optimization of 2D elastic structures using boundary.... Eng Anal Bound Elem (2007), doi:10.1016/j.enganabound.2007.10.003

4. BEM implementation

The implemented algorithm solves the optimization problem incrementally by progressively removing a small portion of the domain per increment (usually known as *hard kill* algorithm [14]). In addition to the constrains introduced in the previous section while presenting the formulation of the topological derivative, it is necessary to consider some additional constraint to the problem in order to avoid the algorithm leading to the trivial solution of the problem, i.e., the complete extinction of the optimization domain. The simplest way to tackle this problem is by introducing a goal minimum material volume fraction, $\gamma_{min} = vol(\Omega^{final})/vol(\Omega^0)$, as stopping criterion.

The algorithm can be summarized as follows (the index j stands for increment number):

(i) Provide an initial domain $\Omega^{j=0}$ and the stopping criterion Fig. 2a.
(ii) Solve the BEM model for the Ω^j domain (Fig. 2b). Compute the stress $\boldsymbol{\sigma}$ and strain $\boldsymbol{\varepsilon}$ fields at internal and boundary points.
(iii) Compute the $D_T(x)$ using the formula (4) or (5).
(iv) Select the points with the minimum values of D_T (a few percent of the total number of points).
(v) Create holes by removing the points selected in step (iv) (Fig. 2c).
(vi) Check stopping criterion. If necessary, make $j = j+1$, define a new domain Ω^j, remesh the BEM model (Fig. 2d) and go to step (ii).
(vii) At this stage the desired final topology is obtained.

4.1. Boundary element analysis

Since the D_T is a function of the stress and strains only, its evaluation does not require any special BEM implementation. Moreover, the recovery of the local D_T value can be easily implemented as a post-processing procedure. The present implementation uses a parallel version of the BEM code SERBA which accompanies the book by Paris and Cañas [15]. The so-called SERBAPA (SERBA PArallel) was coded using message passing interface (MPI) standard and it runs on Beowulf Cluster set up using Linux and built using five Pentium 4 CPUs. It is worth to note that in addition to the computing time improvement for the problem solution, SERBAPA resulted in important time savings in the post processing when computing stresses and strains at internal points. This is due to the important number of internal points used in the model discretization (see Section 4.2).

4.2. Model discretization and remeshing

The model discretization and remeshing strategies are key issues for the performance of the implemented algorithm. The initial BEM model is discretized using two-node linear continuous elements and a regular array of

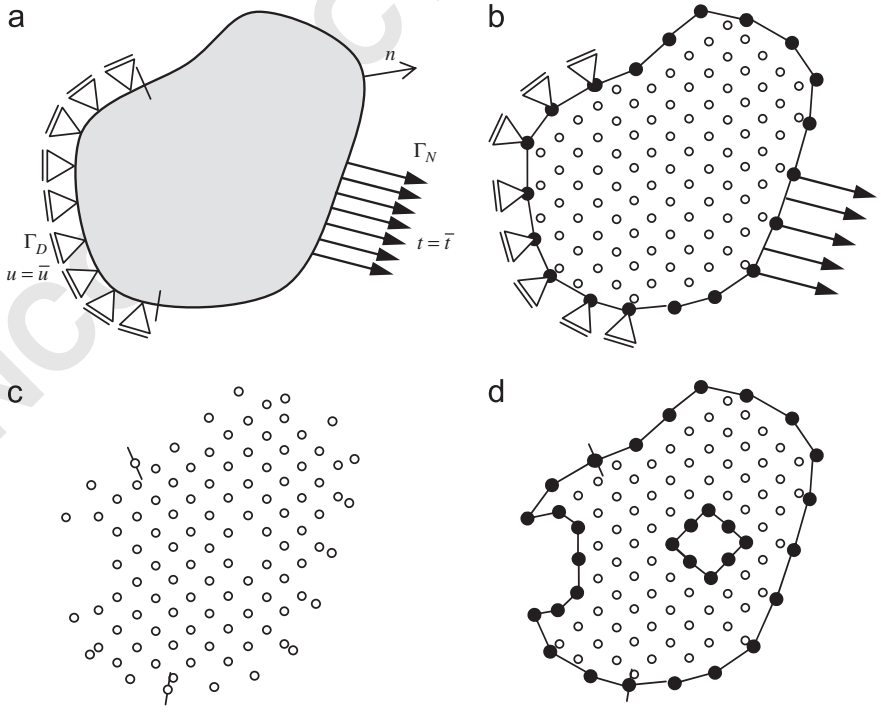

Fig. 2. BEM implementation: (a) problem definition and boundary conditions; (b) initial BEM model; (c) elimination internal points; and (d) BEM model remeshing.

internal points following the pattern depicted in Fig. 2b. The removal of internal and boundary points in every increment is followed by a model remeshing. With this purpose the programme MeshSuite, based on an α-shapes algorithm is employed [16]. Alpha shapes can be viewed as Delaunay triangularization of a point set weighted by the parameter α. Alpha shapes formalize the intuitive notion of shape, and for varying parameter α, it ranges from crude to fine shapes. The most crude shape is the convex hull itself, which is obtained for very large values of α. As α decreases, the shape shrinks and develops cavities that may join to form holes. In this work the parameter α is selected as the average distance between boundary nodes. This is the reason why internal points are distributed on the model domain using a regular array. Upon the input of the coordinates of the boundary nodes and internal points after each optimization step (see Fig. 2c), MeshSuite outputs the connectivity of the new model boundary (see Fig. 2d). Thus, those points not used as boundary nodes are assimilated to internal points in the new discretization.

Depending on the spatial distribution of the points, two problems may arise in the new boundary discretization (see Fig. 3a): (i) a multi-connected boundary points which take part in the connectivity of two (or even more) boundaries; and (ii) there are closed contours defining "islands" disconnected from the main model boundary. Both problems are remedied by simply removing the conflicting points from the model. Multi-connected points are identified after checking that every valid boundary node belongs to the connectivity of two boundary elements only. On the other hand, for the deletion of the disconnected portions of the model it is necessary to test whether a closed contour defines an "island" or a hole. This is done by defining an auxiliary point in the direction of the outward normal to the contour (see point J in Fig. 3a). If it is verified that the auxiliary point is outside the contour the conflicting points constitute an "island" and they are removed. It is worth noting that the two checks mentioned above are performed in every increment of the optimization algorithm. Moreover, the checks are performed repeatedly until no problems are detected, since the

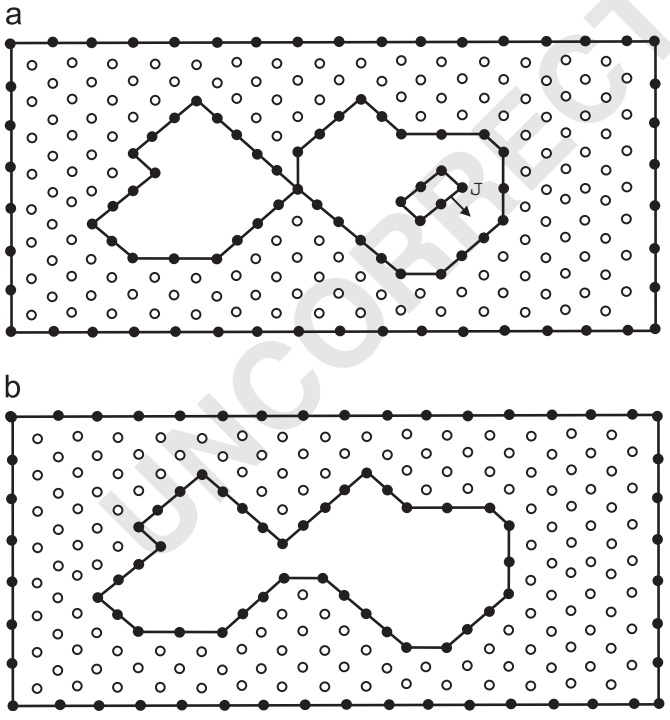

Fig. 3. (a) Problems arising during the automatic model remeshing, multi-connected boundary nodes and "islands" disconnected from the main model boundary; and (b) suitable model discretization after the deletion of the conflicting points.

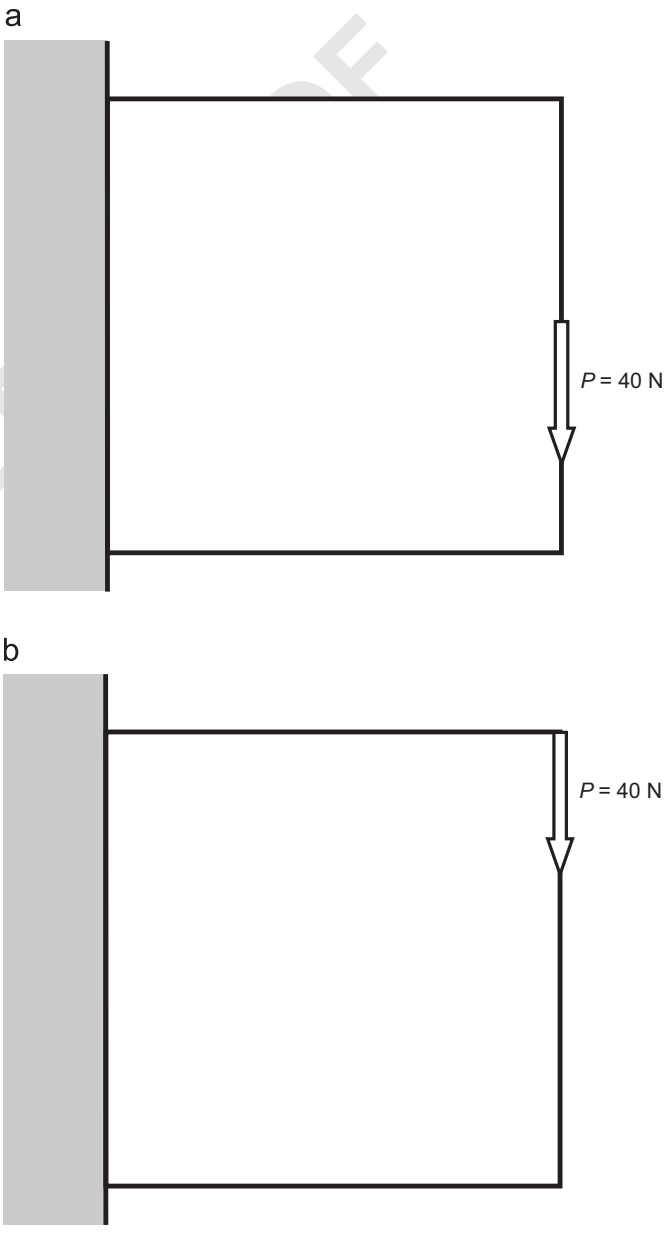

Fig. 4. Geometry for the Examples 1 and 2. Short cantilever beams with loads applied (a) at the middle of the middle and (b) at the top of the free vertical edge.

Please cite this article as: Carretero Neches L, Cisilino A. Topology optimization of 2D elastic structures using boundary.... Eng Anal Bound Elem (2007), doi:10.1016/j.enganabound.2007.10.003

deletion of a point as a consequence of previous checks could lead to the occurrence of new conflicting situations.

5. Examples

Results for four examples are presented in this section. In order to assess the performance of the BEM algorithm, the first three examples are well-known validation examples. The last example is dedicated to an application problem.

For all examples, the material used is steel with modulus of elasticity of 210 GPa and Poisson's ratio $v = 0.3$. All the examples are in plane stress condition.

5.1. Short cantilever beam with load at the middle of the free vertical edge

This first validation example consists in the short cantilever beam illustrated in Fig. 4a. The optimization domain is a square of size 10 m × 10 m, discretized using 400 boundary elements and 9801 internal points following the pattern shown in Fig. 2b. Using this discretization scheme, each internal point and boundary node represents around 0.01% of the initial model domain. The left side of the domain was fixed (zero displacement boundary condition) and a total vertical load $P = 40$ N was applied at the middle of the right side. The load P was applied over a length $d = 0.4$ m (four boundary elements). The specified minimum material volume fraction is $\gamma_{min} = 0.2$.

Two methods were used for setting the rate of material removal. The first one consisted in removing a constant amount of material in every increment, this amount computed as a percentage of the initial model volume, $vol(\Omega^0)$. Using this strategy (which in what follows will be referenced as the "constant method") the problem was solved removing 5%, 1% and 0.2% of the initial model volume in every increment. In the second method the amount of removed material was updated in every increment, that is, the amount of removed material is computed as a percentage of the current model volume, $vol(\Omega^j)$. In this way the actual amount of removed material diminishes with the progress of the optimization process. A percentage of 5% was used when solving the problem using the so-called "updated method".

Fig. 5 displays the evolution of the normalized cost function in terms of the material volume fraction for the three solutions computed using the constant and the updated methods. Besides, Fig. 6 illustrates the intermediate (volume fraction in the range $0.45 \leqslant \gamma_j \leqslant 0.48$) and final geometries (volume fraction $0.20 \leqslant \gamma_j \leqslant 0.23$) obtained using the constant method.

The results in Fig. 5 allow verifying the convergence of the optimization scheme. The three sets of results obtained using the constant method show that the overall value of the cost function diminishes with the reduction of the amount of material removed per increment. At the same time it can be seen that the three sets of results behave similarly up the volume fraction $\gamma \approx 0.50$ (the normalized cost function at this point ranges from $2.02 \leqslant \Psi/\Psi_0 \leqslant 1.88$ for a material removal rates of 5% and 0.2%, respectively), and then start diverging. In essence, the 5% solution starts producing more "expensive" results when compared to 1% and 0.2% removal rates. This observation is in accordance with the geometries illustrated in Fig. 6. The intermediate results show that the 1% and 0.2% geometries respond to the same basic design: two principal "$>$-shape" structures

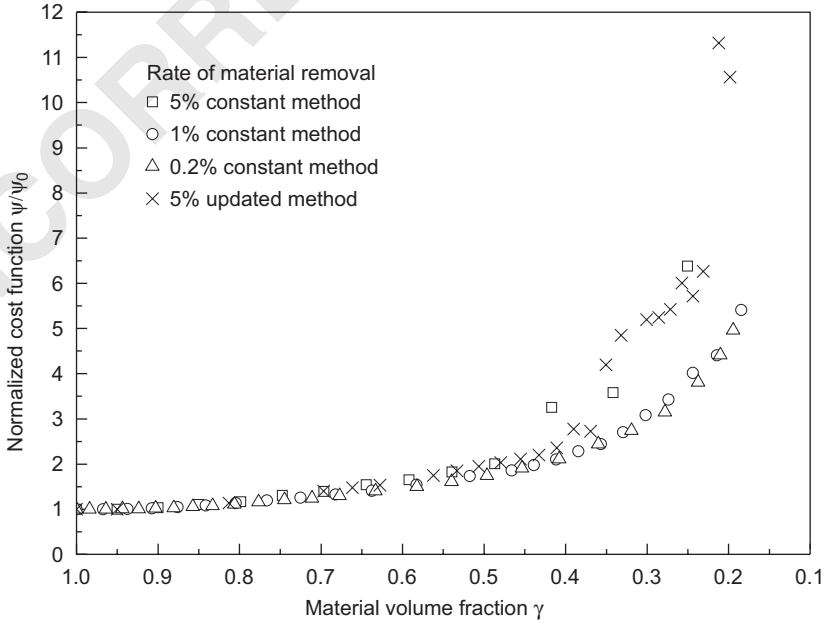

Fig. 5. Example 1: evolution of the normalized cost functions in terms of the material volume fraction.

Please cite this article as: Carretero Neches L, Cisilino A. Topology optimization of 2D elastic structures using boundary.... Eng Anal Bound Elem (2007), doi:10.1016/j.enganabound.2007.10.003

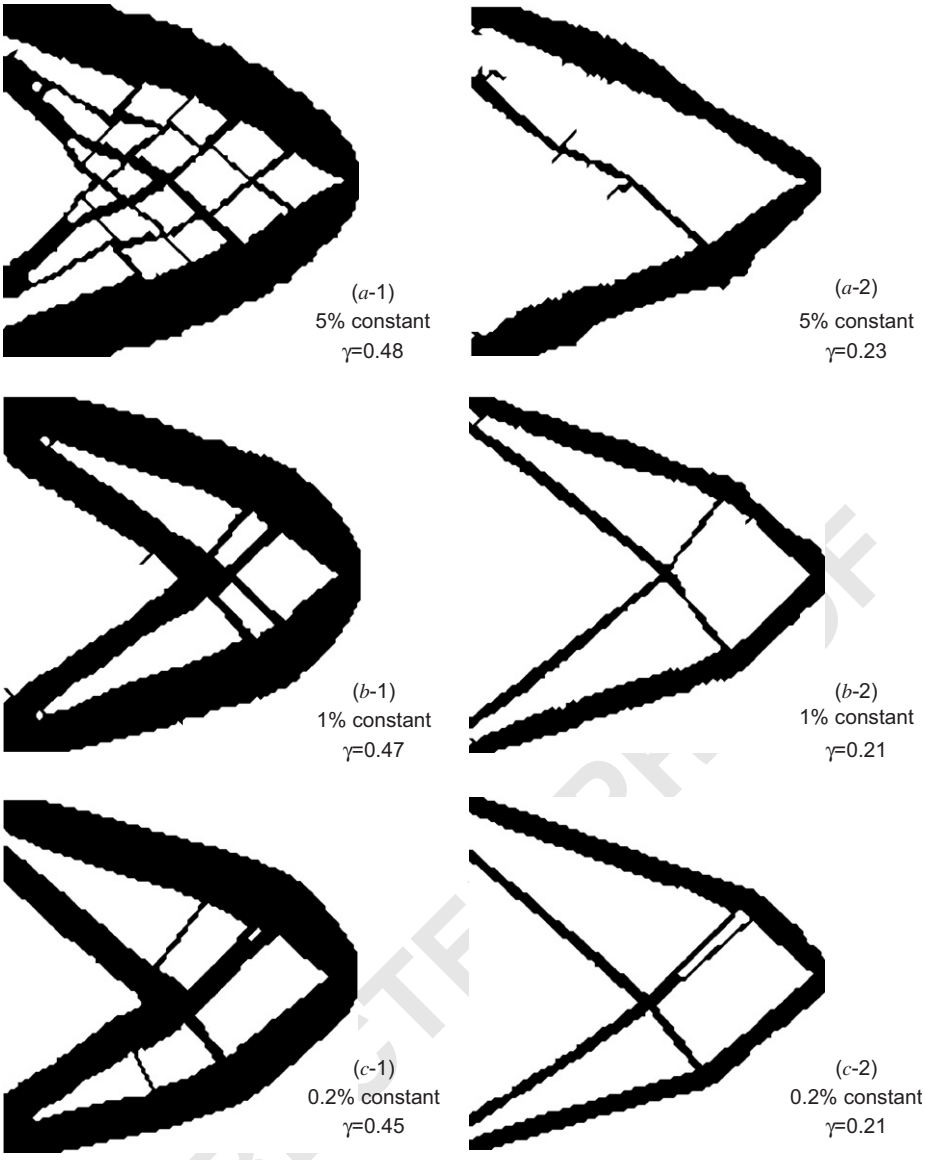

Fig. 6. Example 1: intermediate and final geometries computed using different material removal rates with the constant method.

connected by auxiliary beams (see Figs. 6b-1 and c-1), while the 5% approach produced a different design consisting in a single exterior "$>$-shape" structure with an internal regular lattice (see Fig. 6a-1). Similarly, the final geometries resulting from the 1% and 0.2% solutions are very similar (see Figs. 6b-2 and c-2), and they present a significant improvement in terms of the cost-function minimization when compared to the 5% solution (see Fig. 5).

Fig. 7 depicts the evolution of the model geometry with the material volume fraction computed using the updated method. When compared with the results in Fig. 6, it can be observed that the intermediate geometry for $\gamma = 0.50$ (Fig. 7c) looks like a transition of those obtained using the constant method with material removal rates of 1% and 5% shown in Figs. 6a-1 and b-1 (the new solution combines portions of an interior "$>$-shape" structure with a small lattice). Besides, the normalized cost Ψ/Ψ_0 associated to this geometry is within the range indicated for the constant-method results (see Fig. 5). For the rest of the simulation the cost function presents a similar behaviour to that of the 5% constant-method solution. Moreover, the configurations of the model geometries at $\gamma = 0.21$ (the result corresponding to the specified minimum material volume fraction) posses a similar configuration (see Figs. 6a-1 and 7d).

Finally, the problem was solved using the updated method with a specified minimum material volume fraction $\gamma_{min} = 0.07$. The resulting intermediate geometry for $\gamma = 0.13$ and the final geometry for $\gamma = 0.075$ are illustrated in Figs. 7e and f, respectively. The final solution is in agreement with that obtained by other authors (see for

Please cite this article as: Carretero Neches L, Cisilino A. Topology optimization of 2D elastic structures using boundary.... Eng Anal Bound Elem (2007), doi:10.1016/j.enganabound.2007.10.003

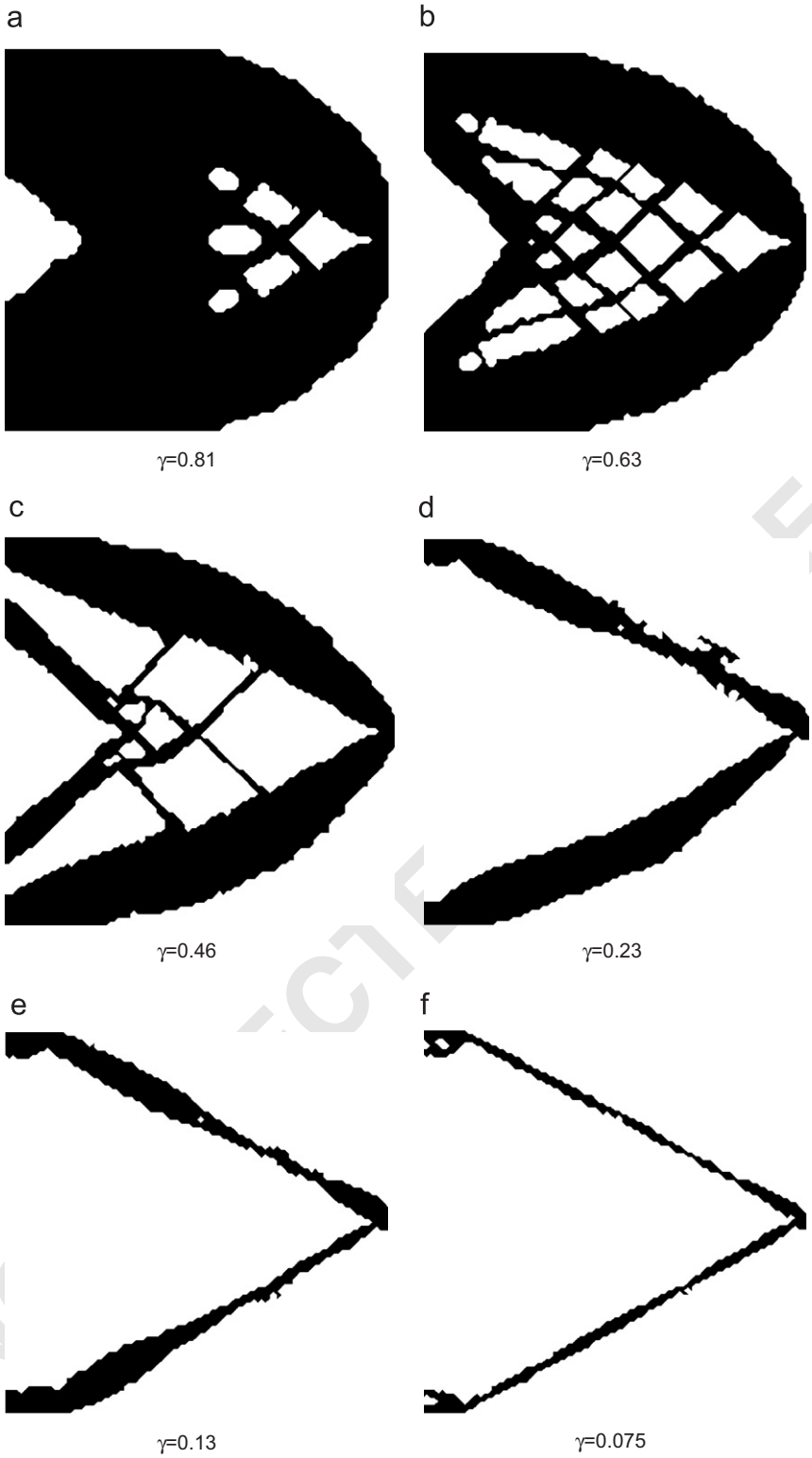

Fig. 7. Example 1: evolution of the model geometry with the material volume fraction. Solution computed using an updated method.

example Ref. [17]). It is worth to mention that updated method was the only capable of achieving such a demanding material volume fraction reduction. All the solutions attempted using the constant method with the above reported material removal rates failed to produce valid models for material volume fractions $\gamma < 0.15$. This is

Please cite this article as: Carretero Neches L, Cisilino A. Topology optimization of 2D elastic structures using boundary.... Eng Anal Bound Elem (2007), doi:10.1016/j.enganabound.2007.10.003

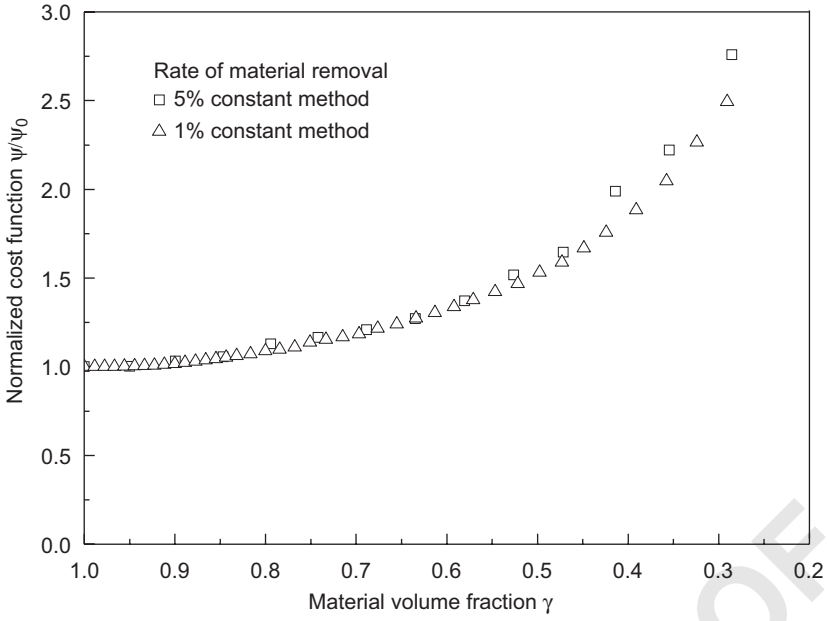

Fig. 8. Example 2: evolution of the normalized cost functions in terms of the material volume fraction.

because at a given stage the algorithm removed an excessive amount of material which resulted in disconnected model geometry.

5.2. Short cantilever beam with the load at the top of the free vertical edge

The geometry of the second validation example is illustrated in Fig. 4b. The problem has the same dimensions, discretization and boundary conditions to that of the first example, with the only exception that the load P is now placed at the top corner of its right edge. Like in the first example the load P was applied over a length $d = 0.4\,\text{m}$ (four boundary elements). The specified minimum material volume fraction is $\gamma_{min} = 0.3$.

Fig. 8 displays the evolution of the normalized cost function in terms of the material volume fraction for both solutions. The problem was solved using the constant method, with material removal rates of 5% and 1%. The results present similar behaviours to those obtained for the first example. The cost functions for both solutions behave almost coincident up a volume fraction $\gamma \approx 0.50$, and then start diverging. The 5% solution produces more "expensive" results than the 1% solution.

The evolution of the problem geometries are depicted in Fig. 9. As it can be seen, both solutions converge to the same final configuration, which is in accordance to that reported by other authors [12,13].

5.3. Michell-type structure

This example consists in the design of a Michell-type structure. This kind of problems is also a usual benchmark for topology optimization algorithms. The initial domain is shown in Fig. 10a. It consists in a rectangle with dimensions $200\,\text{m} \times 100\,\text{m}$ submitted to a distributed constant load $q = 10\,\text{kN/m}$ along the lower edge. Displacement boundary conditions are imposed in order to ensure the model symmetry. The problem was discretized using 600 boundary elements and 19,700 internal points. The problem was solved using the constant method, with a material removal rate of 1%. The specified minimum material volume fraction is $\gamma_{min} = 0.60$.

A number of intermediate and final optimization geometries are shown in Figs. 10b–d. The resultant topology is the classical result for this problem [17].

5.4. Design of a hook

This last example consists in a design of a hook to lift a load. The initial optimization domain is chosen as a rectangular plate with dimensions $100\,\text{mm} \times 150\,\text{mm}$ with a circular hole used to introduce a bolt to connect the hook to the lifting mechanisms, and a slot used access the loading point (see Fig. 11a). The problem was discretized using 783 boundary elements and 22,482 internal points. The problem was solved using the constant method, with a material removal rate of 1%. The specified minimum material volume fraction is $\gamma_{min} = 0.30$.

Figs. 11b–d depict the evolution of the optimization procedure. One the optimization was completed; the

Please cite this article as: Carretero Neches L, Cisilino A. Topology optimization of 2D elastic structures using boundary.... Eng Anal Bound Elem (2007), doi:10.1016/j.enganabound.2007.10.003

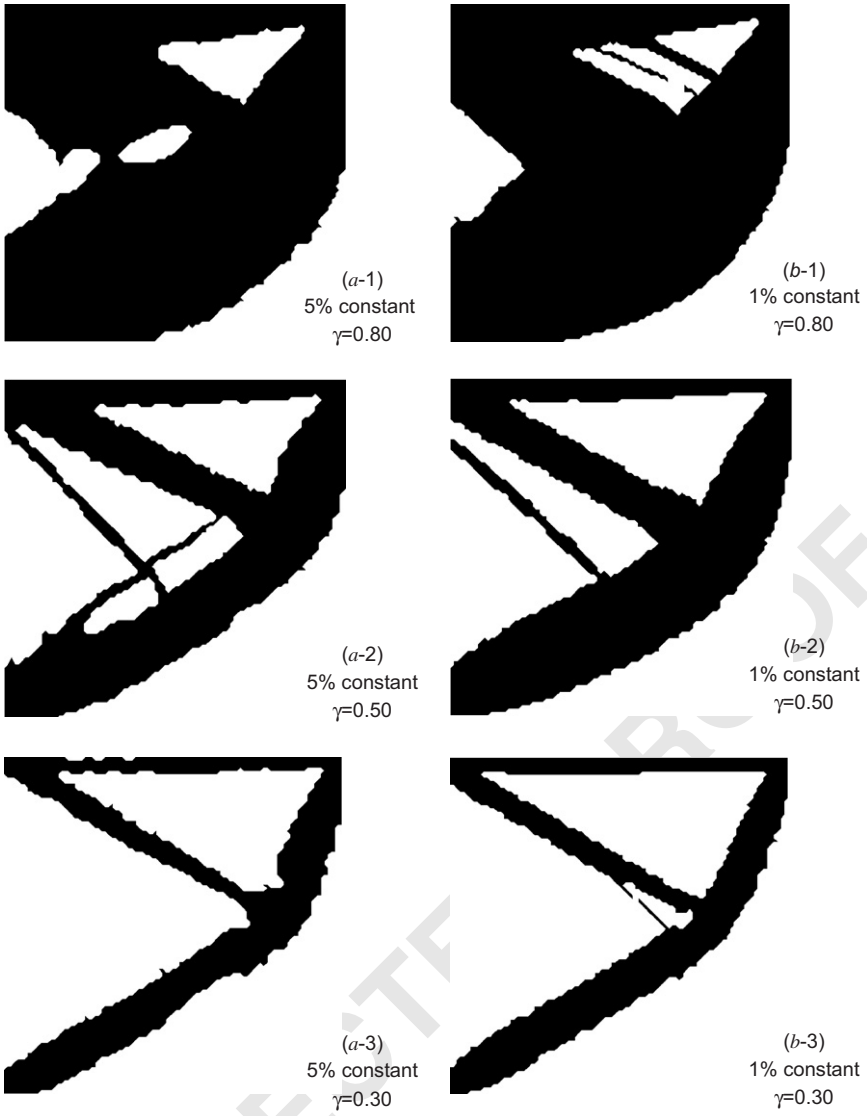

Fig. 9. Example 2: intermediate and final geometries computed using different material removal rates.

resulting geometry was smoothed in order to provide a manufacturable final design (see Fig. 12a). The final design was solved using a new BEM model and the obtained results compared to those of the initial geometry. The normalized cost for the final design is $\Psi/\Psi_0 = 0.7$, while the displacement of the loading point is incremented only 35%.

6. Conclusions

An effective BEM implementation for the topological optimization of 2D elastic structures was presented in this work using the total strain energy as cost function. The problem formulation is based on some recent results by Novotny et al. [13], who introduced a new procedure for computing the topological derivative which allows overcoming some mathematical difficulties involved in its classical definition.

The optimization problem is solved incrementally, by progressively removing a small portion of the domain per increment. BEM models are discretized using linear elements and a regular array of internal points. The topological derivative is computed at boundary nodes and internal points from the strain and stress results. In every step the material removal is done by deleting those internal points and/or boundary nodes with the lowest values of the topological derivative. The material removal is followed by a model remeshing which consists in weighted Delaunay triangularization algorithm and a checking procedure devised to avoid the occurrence of invalid BEM models. The process is repeated until the given stopping criterion (the goal minimum material volume fraction) is achieved.

Please cite this article as: Carretero Neches L, Cisilino A. Topology optimization of 2D elastic structures using boundary.... Eng Anal Bound Elem (2007), doi:10.1016/j.enganabound.2007.10.003

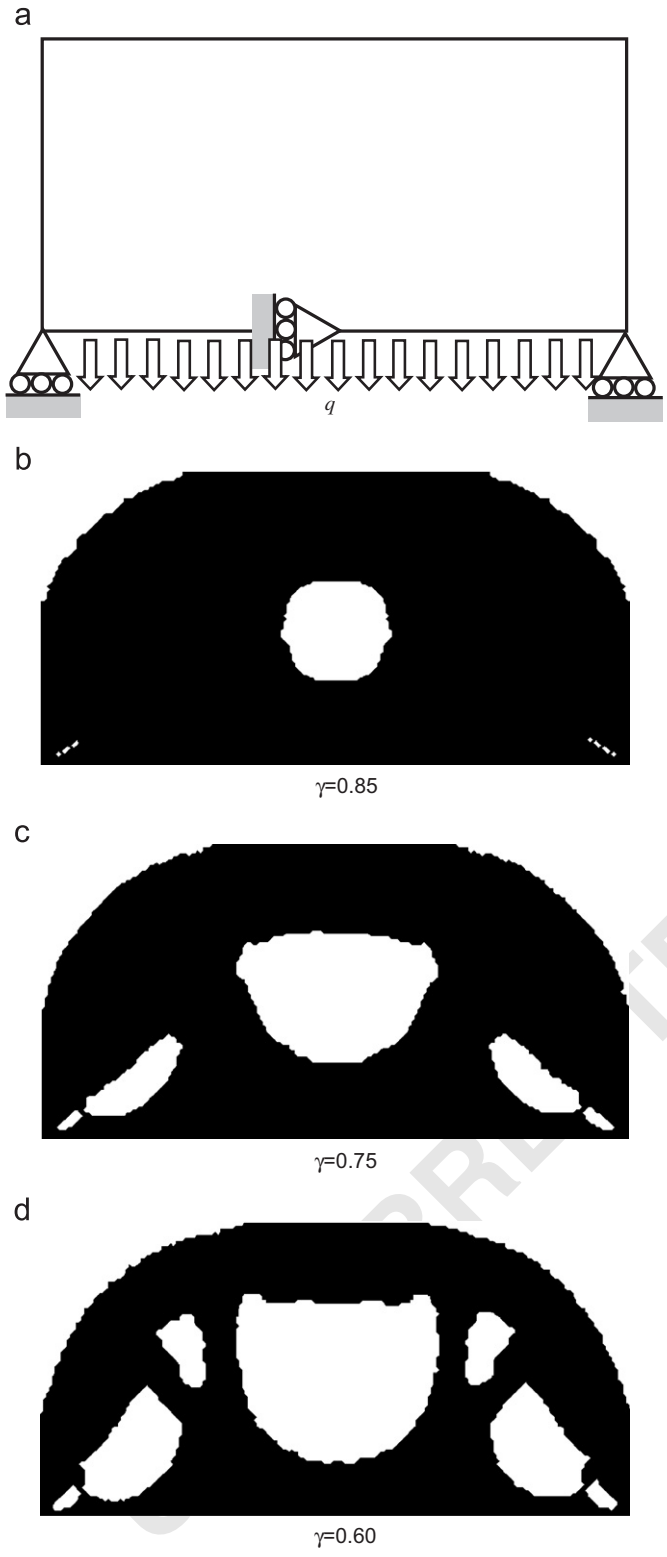

Fig. 10. Michell-type structure: (a) initial problem geometry and (b–d) boundary conditions and evolution of the geometry with the material volume fraction.

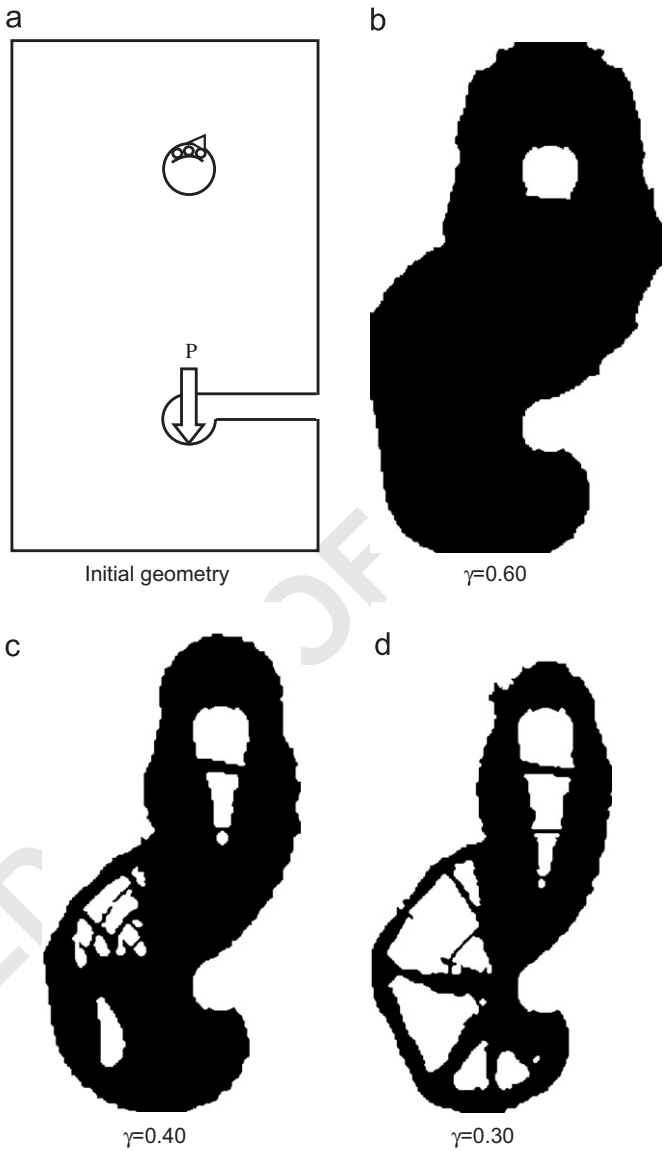

Fig. 11. Design of a hook: (a) initial geometry for the hook and (b–d) evolution of the model geometry with the material volume fraction.

Two methods were used for setting the rate of material removal: (i) a constant amount of material per increment given as a percentage of the initial model volume, and (ii) an updated amount of material given as a percentage of the current model volume. The convergence analysis of the cost function indicates that for the constant method a material removal per increment equal to 1% is enough to produce results independent of the material removal rate. Besides, the constant method failed to produce geometries with volumes less than 15% of the initial geometry volume. Although it can be argued that this limitation of the constant method can be tackled by using finer discretizations and smaller material removal rates, this alternative is not convenient in terms of computing cost. On the other hand, the updated method allows achieving geometries with final volumes only a few percent of the initial one.

Please cite this article as: Carretero Neches L, Cisilino A. Topology optimization of 2D elastic structures using boundary.... Eng Anal Bound Elem (2007), doi:10.1016/j.enganabound.2007.10.003

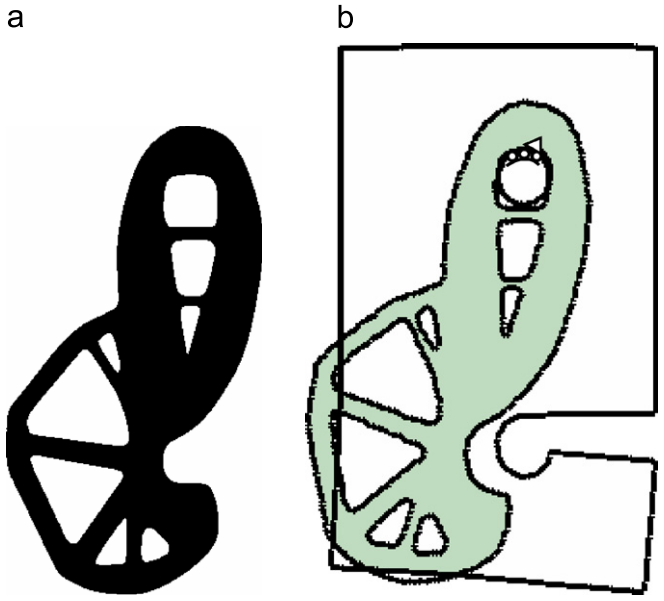

Fig. 12. Design of a hook: (a) final design and (b) comparison of the displaced configurations for the initial and final designs (displacements are magnified 50 times).

The proposed method proves to be efficient and robust. Its performance is assessed by solving a number of benchmark problems and an application example.

Acknowledgements

The authors wish to express their gratitude to N. Calvo (CIMEC, Argentina) for providing the MeshSuite software used for the automatic BEM model discretization. This work has been partially supported by the Agencia de Promoción Científica de la República Argentina under Grants PICT 12-14114 and PICT 12-12528 and the ALFA Project ELBENET "Europe-Latin America Boundary Element Network" sponsored by the European Union.

References

[1] Ceá J, Garreau S, Guillaume P, Masmoudi M. The shape and topological optimization connection. Comput Methods Appl Mech Eng 2000;188:713–26.

[2] Tanskanen P. The evolutionary structural optimization method: theoretical aspects. Comput Methods Appl Math Eng 2002;190:4081–193.

[3] Bensoe MP, Kikuchi N. Generating optimal topologies in structural design using a homogenization method. Comput Methods Appl Mech Eng 1988;71:197–224.

[4] Sigmund O, Peterson J. Numerical instabilities in topology optimization: a survey on procedures dealing with checkerboards, mesh dependencies and local minima. Struct Optim 1998;16:68–75.

[5] Wang MY, Wang X. PDE-driven level sets, shape sensitivity and curvature flow for structural topology optimization. Comput Methods Eng Sci 2004;6(4):373–95.

[6] Wang MY, Wang X. Structural shape and topology optimization using an implicit free boundary parametrization method. Comput Methods Eng Sci 2006;13(2):119–47.

[7] Ceá J, Gioan A, Michel J. Adaptation de la méthode du gradient a a un probleme d'idenfification de domaine. In: Lecture Notes in Computer Science, vol. 11. Springer: Berlin; 1974. p. 371–402.

[8] Novotny AA, Feijoo RA, Taroco E, Padra CC. Topological sensitivity analysis. Comput Methods Appl Mech Eng 2003;192:803–29.

[9] Mackerle R. Topology and shape optimization of structures using FEM and BEM—a bibliography (1999–2001). Finite Elem Anal Des 2003;39:243–53.

[10] Cisilino AP. Topology optimization of 2D potential problems using boundary elements. Comput Model Eng Sci 2006;15(2):99–106.

[11] Marckzak RJ. Topology optimization and boundary elements—a preliminary implementation for linear heat transfer. Eng Anal Bound Elem (the paper is available on line at the moment of the preparation of this manuscript), to appear. Q1

[12] Marckzak RJ. A boundary element implementation for topology optimization of elastic structures. In: Proceedings of the XXVII Iberian Latin-American congress on computational methods in engineering CILAMCE 2006, Belem, Brazil, 2006.

[13] Novotny AA, Feijoo RA, Padra CC, Taroco E. The topological-shape sensitivity analysis and its applications in optimal design. Mecanica Computacional XXI. In: Idelsohn SR, Sonzogni VE, Cardona A, editors. Proceeding of the First South American Congress on computational mechanics. Santa Fe, Argentina, 2002.

[14] Eschenauer HA, Olhoff N. Topology optimization of continuum structures: a review. Appl Mech Rev 2001;54:331–90.

[15] Paris F, Cañas J. Boundary element method: fundamentals and applications. USA: Oxford Science Publications; 1997.

[16] Calvo N, Idelsohn SR, Oñate E. The extended Delaunay tessellation. Eng Computations 2003;20(5–6).

[17] Wang MY, Wang X, Guo D. A level set method for structural topology optimization. Comput Methods Appl Mech Eng 2003;192:227–46.